HHS Public Access

Author manuscript

Nanoscale. Author manuscript; available in PMC 2019 July 05.

Published in final edited form as:

Nanoscale. 2018 July 05; 10(25): 11841–11849. doi:10.1039/c8nr01646a.

Nanoparticle-enhanced electrical detection of Zika virus on paper microchip

Mohamed Shehata Draz[a,b,c], **Manasa Venkataramani**[a,†], **Harini Lakshminarayanan**[a,†], **Ecem Saygili**[a,†], **Maryam Moazeni**[a], **Anish Vasan**[a], **Yudong Li**[a], **Xiaoming Sun**[d], **Stephane Hua**[d], **Xu G. Yu**[d,e], and **Hadi Shafiee**[a,b,*]

[a]Division of Engineering in Medicine, Department of Medicine, Brigham and Women's Hospital, Harvard Medical School, Boston, Massachusetts 02115

[b]Department of Medicine, Harvard Medical School, Boston, MA 02115, USA

[c]Faculty of Science, Tanta University, Tanta 31527, Egypt

[d]The Ragon Institute of Massachusetts General Hospital, Massachusetts Institute of Technology and Harvard University, Boston, MA 02129

[e]Division of Infectious Diseases, Department of Medicine, Brigham and Women's Hospital, Harvard Medical School, Boston, Massachusetts 02115

Abstract

Zika virus (ZIKV) is a reemerging flavivirus causing an ongoing pandemic and public health emergency worldwide. There are currently no effective vaccines for Zika infection or specific therapy. Rapid, low-cost diagnostics for mass screening and early detection is of paramount importance in timely management of the infection at the point-of-care (POC). The current Zika diagnostics are laboratory-based and cannot be implemented at the POC particularly in resource-limited settings. Here, we developed a nanoparticle-enhanced viral lysate electrical sensing assay for Zika virus detection on paper microchips with printed electrodes. The virus is isolated from biological samples using antibodies and labeled with platinum nanoparticles (PtNPs) to enhance the electrical signal. The captured ZIKV-PtNPs complexes are lysed using a detergent to release the electrically charged molecules associated with the intact virus and the PtNPs on the captured viruses. The released charged molecules and PtNPs change the electrical conductivity of the solution, which can be measured on a cellulose paper microchip with screen-printed microelectrodes. The results confirmed a highly specific detection of ZIKV in the presence of other non-targeted viruses, including closely related flaviviruses such as Dengue-1 and Dengue-2 with a detection limit down to 10^1 virus particle/μl. The developed assay is simple, rapid, and cost-effective and has the potential for POC diagnosis of viral infections and treatment monitoring.

*Corresponding author. hshafiee@bwh.harvard.edu.
†Authors contributed equally to this work

Conflicts of interest

There are no conflicts to declare.

Introduction

Zika virus (ZIKV) is a member of the Flaviviridae, which was initially limited to sporadic cases in Africa and Asia. Recently, ZIKV infection poses a serious pandemic threat to more than 33 countries worldwide causing a myriad of neurologic disorders, which have drastic consequences in newborns[1–6]. The clinical manifestations of Zika viral infection are similar to that of other arboviral infections. In addition, the current diagnostic techniques available for ZIKV are based on reverse transcription-polymerase chain reaction (RT-PCR)[7–10] for nucleic acid detection or enzyme-linked immunosorbent assay (ELISA)[11–14] for detecting antibodies developed against the virus. The presence of secondary antibodies from other Flaviviral infections leads to cross-reactivity in ELISA-based tests. Nucleic acid detection is also limited by short time course of infection and technically time-consuming and expensive.[15–18] Thus, the detection of intact virus particles can potentially offer a better alternative for direct viral load testing without the cross-reactivity of antibodies.

Cellulose paper microchips and electrical sensing are gaining a wide reputation for developing flexible, low-cost point-of-care (POC) diagnostics.[19,20] Paper microchips have become increasingly attractive by offering many advantages for biosensing, including flexibility, portability, simple fabrication and modification, low-cost manufacturing, biodegradability, minimal consumption of sample and reagents, and multiplexing.[21–23] On the other hand, electrical sensing as a detection modality is simple and sensitive and does not require bulky components that are usually used in optical and fluorescence-based assays, which makes it one of the most common sensing modalities used in the development of POC devices.[24–26] So far numerous systems that integrate electrical sensing and paper microfluidics have been developed for the detection of different diseases and infections, including human immunodeficiency virus (HIV), hepatitis B virus (HBV), *Escherichia coli*, methicillin-resistant *Staphylococcus aureus* (MRSA) and different cancer biomarkers.[27–32]

Nanoparticles exhibit versatile optical, electrical, and catalytic properties for diagnostic and therapeutic applications.[33,34] Among different types of nanoparticles, metal nanoparticles such as Au, Ag, Cu, Fe, and Pt have been widely used in chemical and biological sensing. Metal nanostructures and composites are easy-to-prepare and characterize, and have considerable stability and biocompatibility allowing their integration with various biosensing modalities, including optical, fluorescence, electrochemical, and electrical sensing.[35,36] Of particular interest in electrical sensing is metal nanoparticles that have been widely described as electroactive and catalytic materials to label target molecules for signal amplification[1].[37–39] Here, we report a nanoparticle-enhanced electrical sensing approach that integrates viral lysate impedance spectroscopy and paper microfluidics using platinum nanoprobes. Virus labeling using metal nanoprobes (*i.e.*, Pt-nanoprobes) improves the sensitivity and specificity of the detection by increasing the conductivity of the produced viral lysate for a given viral load. We evaluated the performance of the developed assay for the specific detection of ZIKV in 1× PBS, plasma, urine, and semen samples. Our results showed that the developed mechanism effectively detect ZIKV with a detection limit of 10^1 copies/μl. The specificity of the device was evaluated using closely related flaviviruses such as Dengue-1 (DENV-1), Dengue-2 (DENV-2), Cytomegalovirus (CMV), and herpes simplex virus (HSV).

Results and Discussion

We report the development of a paper microchip with printed electrodes for ZIKV detection using nanoparticle-enhanced electrical sensing modality. This approach primarily integrates three technologies in signal amplification using PtNPs conjugated with antibodies, viral lysate impedance spectroscopy, and cellulose paper microchip fabrication to allow sensitive and highly specific detection of virus particles (Figure 1a). The virus particles are initially captured on the surface of magnetic beads modified with anti-Zika virus monoclonal antibody (anti-ZIKV mAb) specifically targeting the envelope protein and labeled using specifically designed Pt-nanoprobes. The Pt-nanoprobes are mainly comprised of spherical PtNPs modified with anti-ZIKV mAb to allow specific interaction and assembly of PtNPs on the virus envelope. The formed PtNP-virus complexes were separated through magnetic separation and the enriched viruses were lysed to release the electrically charged virus components including nucleic acid and proteins along with PtNPs in the solution. The electrical conductivity of the solution was then measured through impedance spectroscopy on paper microchips with printed flexible electrodes. The electrical properties of PtNPs as metal nanostructures help in enhancing the signal. In the absence of ZIKV particles, neither virus particles components nor PtNPs exist in the lysis products and tested samples possess impedance magnitudes that are significantly different than the virus-free control samples (Figure 1b).

The preparation protocol for Pt-nanoprobes relies on using a bifunctional crosslinker of 3-(2-pyridyldithio)propionyl hydrazide (PDPH) to allow a directional conjugation of antibodies to the surface of nanoparticles (Figure 2a). The reduced PDPH molecules bind to the metallic surface of PtNPs through their terminal thiol group forming PtNPs carrying hydrazide groups. The free hydrazide groups can react with the carbohydrate residues in the FC region of antibodies oxidized by sodium periodate. Figures 2a and S1 show the detailed conjugation protocol used in the preparation of Pt-nanoprobes. Figure 2b shows the transmission electron microscopy (TEM) and the corresponding size distribution histogram that confirm that the prepared PtNPs were spherical in shape with an average diameter of 3.9±0.5 nm. Dynamic light scattering (DLS) and zeta potential techniques confirmed the stability of the formed PtNPs with an average diameter of 9.9±0.1 nm and negative surface charge of -14.1±0.6 (Figure S2, 3). To confirm the conjugation of anti-ZIKV mAb to the surface of PtNPs and the formation of stable Pt-nanoprobes, the Pt-nanoprobes were characterized using Fourier-transform infrared spectroscopy (FT-IR) and sodium dodecyl sulfate polyacrylamide gel electrophoresis (SDS-PAGE) techniques. Figures 2c and S4 indicate a considerable similarity between the FTIR spectra of the prepared Pt-nanoprobes and control sample of anti-ZIKV mAb. The bands appearing at 1720.56 cm^{-1}, 1448.58 cm^{-1}, 1103.31 cm^{-1}, 977.94 cm^{-1}, and 837.13 cm^{-1} can be contributed to C=O stretching, N–H bending, C–N stretching, C–C stretching, and S-metal bond, respectively.[40] These bands correspond to the thiol-Pt bond formed by PDPH with the surface PtNPs and to amid-I and -II characteristic to antibodies coupled to the surface of the PtNPs. On the other hand, SDS-PAGE results shown in Figure 2d indicate the presence of two protein bands at 50 kDa and 25 kDa for samples prepared with Pt-nanoprobes.[41] These two protein bands are

characteristics of the light and heavy chains of IgG and are similar to the bands that appeared in the control samples of anti-ZIKV mAb without the presence of PtNPs.

The developed paper microchip comprises of a cellulose paper substrate assembled together with a thin transparent plastic sheet by double-sided adhesive (DSA). The fabrication process of the cellulose paper microchip is simple and can be completed in < 1 h (manually) following layer-by-layer assembly of plastic and cellulose substrates and screen-printing electrodes (Figure 3a). A sheet of cellulose paper (0.34 mm in thickness) was sandwiched between a masking sheet and DSA and patterned through laser cutting to form the required space for electrode printing. The machined mask-cellulose paper-DSA was sealed with a thin sheet of plastic (0.1 mm in thickness). Then, 4-finger–like interdigitated electrode was screen-printed using preoptimized graphene-modified silver nanocomposite ink.[27] The digital image in Figure 3b shows the front and back view of a fabricated paper chip. The structure of the chip was characterized using optical and scanning electron microscopy (SEM). Transverse and surface sections of freshly prepared chips showed the layer structure of the printed electrodes (Figure 3ci, ii). The screen-printed electrode layers were diffused within the cellulose paper with high resolution, allowing enhanced and efficient contact with the surface cellulose paper layer. In addition, we evaluated the performance of the cellulose paper electrodes by impedance spectroscopy using different dilutions from phosphate buffer saline (1× PBS, pH 7.2). The impedance spectroscopy of 100%, 50%, 10%, 1%, 0.1% and 0% PBS samples diluted in DI water for frequencies between 1 to 20 KHz and 1 V are shown in Figure 3d. The results showed that the microchip can be used to differentiate between different concentrations of PBS samples using impendence spectroscopy.

The capture of ZIKV particles on the surface of magnetic beads and the post-labeling step with Pt-nanoprobes were confirmed using SDS-PAGE and inductively coupled plasma-mass spectrometry (ICP-MS), respectively. The results of SDS-PAGE analysis show the presence of several protein bands at 50 kDa and 25 kDa that are characteristics to monoclonal antibodies and a major band around 79 kDa that is characteristic for the NS3 protein of ZIKV (Figure 3e).[42] On the other hand, ICP-MS confirmed the accumulation of Pt metal on the surface of beads in the presence of ZIKV particles, while in the absence of ZIKV the detected concentration of Pt metal was < 0.01 μg/ml, which is similar to control samples of non-modified magnetic beads (Figure 3f).

The detection sensitivity and specificity of the system were tested using the target ZIKV and non-target viruses, including dengue virus (DENV) type-1 and -2, cytomegalovirus (CMV), and herpes simplex virus-1 (HSV-1). ZIKV particles in different concentrations (10° particle/μl to 10^5 particle/μl) prepared in 1× PBS with pH of 7.2 were captured on magnetic beads and lysed using 1% Triton X-100 solution. The prepared viral lysates were loaded on 4-finger paper electrodes and tested using an LCR meter for impedance measurement at 8000 Hz and 1 V. The results indicated that the tested virus concentration and impedance magnitudes were inversely proportional and with the increase in the tested virus concentrations, the impedance magnitude decreased. This could be attributed to the increase in the concentration of the released charged molecules (*i.e.*, viral nucleic acid and proteins) and PtNPs in the lysis products with the increase in virus concentrations (Figure 4a). The developed assay showed a detection limit down to 10^1 particle/μl of ZIKV in PBS,

considering signal-to-noise ration (S/N) = 3 compared to virus-free control. On the other hand, the detection specificity of this assay was confirmed by testing samples of ZIKV and non-target viruses (*i.e.*, DENV-1, DENV-2, CMV, HSV-1) at virus concentration of 10^5 particle/μl. The impedance magnitude generated from the target ZIKV was at least 3-times lower than the impendence magnitudes generated from all other non-target viruses tested (n = 3, P<0.001) (Figure 4c).

The potential of the developed NP-electrical impedance assay for the detection of ZIKV in more complex biological samples including human plasma, semen, and urine was evaluated using samples with different virus concentrations (*i.e.*, 10^1 particle/μl, 10^2 particle/μl, 10^3 particle/μl, 10^4 particle/μl, and 10^5 particle/μl) (See methods). The isolated virus particles were labeled using Pt-nanoprobes and detected on paper microchips through electrical sensing of viral lysate. The obtained impedance magnitudes indicated that the increase in the virus concentration results in a significant decrease in the impedance magnitude measured at 8000 Hz and 1 V (Figure 5 a-c). Furthermore, the detection limit of the developed assay for the detection of ZIKV spiked in plasma, semen, and urine was 10^2 particle/μl, considering S/N = 3. In the meanwhile, no obvious change in the impedance magnitude was observed from virus-free control samples. These results confirm that the developed NP-electrical impedance sensing mechanism has the potential to be applied to detect ZIKV in the clinical and patient samples.

Experimental

Microchip Fabrication

The microchip was fabricated using cellulose paper substrate with 0.34 mm thickness (Whatman 3MM Chromatography paper, Whatman™ 30306185, Fisher Scientific). For electrode screen-printing, the cellulose paper was covered with a masking paper (Mask-ease, Blick Art Materials; 44908-1003) on the upper surface and with a 80 μm-thick double-sided adhesive (DSA) on the lower surface. This was then machined with laser cutter (Laser Cutting, VLS2.30 from Universal Laser System) to prepare finger-like integrated electrodes with 2 mm width and spacing. The power, scan speed, and pulse per inch rate were set at 11 W, 5 mm/s, and 500 respectively, with the laser at a height of 3.175 mm. After removing the protective layer from the other side of the DSA, the paper was attached to a thin plastic sheet (CG5000 - Dual-Purpose Transparency Film) that is 0.1 mm thick. Silver-graphene nanocomposite ink was prepared by mixing graphene conductive dispersion (Graphene Supermarket, UHC-NPD-100ML) and silver ink (Engineered Conductive Materials, CI-1001) with a ratio of 4:1 and used for screen-printing. The printed electrodes were allowed to dry for less than an hour in an oven at 65 ^{o}C.

Pt-nanoprobes preparation and characterization

Pt-nanoprobes used in the labeling step of captured ZIKV were prepared of spherical platinum nanoparticles (PtNPs) modified with monoclonal anti-Zika virus (ZIKV-Env) antibody (EastCoast Bio, Inc. North Berwick, ME, USA, Cat# HM325). First, citrate-capped PtNPs were synthesized using a previously published protocol.[43] The prepared PtNPs were modified with 3-(2-pyridyldithio)propionyl hydrazide (PDPH) that is freshly reduced by 20

mM tris(2-carboxyethyl)phosphine (TCEP). For antibody coupling reaction, aliquots of 5 μl of antibody (9 mg/ml) were mixed with 10 mM of sodium metaperiodate and 0.1 M sodium acetate (pH 5.5) and incubated at 4°C in dark for 20 min. Then, the oxidized antibody was added to PDPH activated PtNPs and allowed to react with the oxidized antibody for 1 h at 25 °C. The prepared PtNPs and Pt-nanoprobes were characterized using transmission electron microscopy (TEM), Ultra violet visible (UV-vis) spectroscopy, Fourier transform-infrared spectroscopy (FT-IR), Zeta potential (ζ), and dynamic light scattering (DLS).

Virus capture and labeling with Pt-nanoprobes—Aliquots of magnetic beads modified with anti-Zika virus monoclonal antibody (anti-ZIKV mAb) were dispensed in a microcentrifuge tube and the supernatant was removed using a MagnaGrIPTM (MilliPore) magnetic stand and replaced with 50 μl of ZIKV samples or control (1× PBS buffer, pH 7.2 with no ZIKV). This sample-bead mixture was incubated on a shaker (250 rpm/min) for 30 min at 25 °C. After incubation, the captured virus was mixed with 50 μl of Pt-nanoprobe solution and incubated for 30 min. The formed Pt-virus-bead complexes were washed 4 times using 10% (v/v) glycerol solution using a fresh tube after each wash.

Virus lysate preparation and electrical testing on-chip

The captured and isolated ZIKV particles and Pt-nanoprobes were lysed in 50 μl of 1% (v/v) Triton X-100 solution for 5 min. 8 μl of the lysate was loaded on the microchip and impedance magnitudes were recorded using an LCR Meter (LCR8110G, GWInstek, CA) at a frequency of 8000 Hz and 1V.

Spiked sample preparation and testing

Plasma was prepared by centrifuging 10 ml fresh whole blood (Research Blood Components, LLC, Brighton, MA, USA) at 2500 rpm for 15 min while semen samples were purchased from California Cryobank Inc., Los Angeles, CA, and USA. ZIKV samples were prepared with final virus concentrations of 10^1 particle/μl, 10^2 particle/μl, 10^3 particle/μl, 10^4 particle/μl, and 10^5 particle/μl. Each spiked sample was tested using the developed paper microchip using the previously described protocol for electrical sensing.

Statistical analyses

The collected data were analyzed using OriginPro 2015 (OriginLab Corporation, Northampton, USA) and GraphPad Prism software version 5.01 (GraphPad Software, Inc. La Jolla, CA, USA). Each data point represents the average of a total of three independent measurements.

Conclusions

This work has demonstrated the development of impedance electrical sensing assay for sensitive and specific detection of ZIKV lysate on paper microchip. This is the first study of integrating PtNPs with paper microfluidics for virus lysate detection to improve electrical sensing of viruses. The Pt-nanoprobes were specifically designed to have ultra-small metallic core of ~4-nm PtNPs and dense surface layer of monoclonal antibodies for capturing ZIKV particles. The relatively small size of PtNPs allowed efficient labeling of the

surface of ZIKV particles with a diameter of approximately 50 nm. In addition, the 4-nm PtNPs are comparable in size to viral proteins and nucleic acid and they would act as small charged molecules that easily flow and migrate within the paper chip matrix (with pore size of 1μm), allowing rapid and efficient electrical signal detection. Furthermore, the antibody conjugation to the surface of PtNPs for Pt-nanoprobes preparation was performed using a multistep protocol that allows directional binding of antibody molecules through their FC region. The directional conjugation of antibodies preserves the full activity of antibodies and allows highly specific interaction with the target with high avidity. Generally, the integration of PtNP-based labeling with viral lysate electrical sensing has the following advantages: 1) It allows an enhanced detection sensitivity that is at least 10-times higher than the direct lysate virus sensing (without Pt-nanoprobes addition) (Figure S5). 2) It improves the specificity and reliability of the detection by limiting the false positive results. This is of particular importance for ZIKV infection where immuno-based detections of ZIKV are usually limited with cross-reactivity with closely related flaviviruses. 3) It allows the detection of relatively small sized viruses such as ZIKV, which is a limitation of the viral lysate electrical sensing approach.

Furthermore, we developed the paper chip using chromatography paper substrates with 0.34mm thickness to increase the volume of the loaded sample and to reduce the sample evaporation rate on-chip, which allowed efficient and stable impedance signal measurement (~1 min). In addition, such thick surface layer of paper allows better diffusion and contact with the surface of the electrodes that are screen-printed within the paper layer of the chip. The material cost to perform one test with the presented approach is less than $2 including 6 cents for the paper, 2 cents for the plastic sheet, less than 1 cent for DSA, 10 cents for the electrodes, 80 cents for magnetic beads, and less than 1 dollar for antibodies. This cellulose paper-plastic-based system have several advantages over other paper-based or plastic-based systems previously developed for electrical sensing including improved contact between the printed electrodes and the cellulose substrate, increased detection area exists between the printed electrodes and the sample due to the fact that conductive inks do not fully develop in the cellulose paper and reduced non-specific interaction due to surface hydrophobicity in plastics. Compared to recently reported paper-based assays for virus detection, our assay is simple, sensitive and can be used for viral load testing without the need to nucleic acid amplification (Table S1).

We have demonstrated the feasibility of the developed NP-electrical sensing-based mechanism for ZIKV detection in human plasma, urine, and semen samples. The reported sensing mechanism has a great potential and can be applied using different types of metal nanoparticles (such as gold and silver nanoparticles) and electroactive nanostructures for broad applications in microbial infection screening and treatment monitoring at the POC.

Supplementary Material

Refer to Web version on PubMed Central for supplementary material.

Acknowledgments

Research reported in this publication was partially supported by the National Institute of Health under award numbers R01AI118502, R21HD092828, and P30ES000002; Harvard T.H. Chan School of Public Health, Harvard Center for Environmental Health through Harvard NIEHS Grant; and American Board of Obstetrics and Gynecology, American College of Obstetricians and Gynecologists, American Society for Reproductive Medicine, Society for Reproductive Endocrinology and Infertility through ASRM Award, Harvard University Center for AIDS Research (CFAR) under award number 5P30AI060354-14, and the Ragon Institute of MGH, MIT and Harvard University through their support to Dr. Xu G. Yu. .

References

1. Marquezan MC, Ventura CV, Sheffield JS, Golden WC, Omiadze R, Belfort R, May W. Surv Ophthalmol. 2018; 63:166–173. [PubMed: 28623165]
2. Nascimento OJM, da Silva IRF. Curr Opin Neurol. 2017; 30:500–507. [PubMed: 28617719]
3. Leal MC, van der Linden V, Bezerra TP, de Valois L, Borges ACG, Antunes MMC, Brandt KG, Moura CX, Rodrigues LC, Ximenes CR. Emerg Infect Dis. 2017; 23:1253–1259. [PubMed: 28604336]
4. Wiwanitkit V. Eur J Intern Med. 2018; 47:e17. [PubMed: 28610843]
5. Mehrjardi MZ. Virology (Auckl). 2017; 8:1178122X17708993.
6. Coyne CB, Lazear HM. Nat Rev Microbiol. 2016; 14:707–715. [PubMed: 27573577]
7. Chan JFW, Yip CCY, Tee KM, Zhu Z, Tsang JOL, Chik KKH, Tsang TGW, Chan CCS, Poon VKM, Sridhar S, Yin F, Hung IFN, Chau SKY, Zhang AJ, Chan KH, Yuen KY. Trop Med Int Heal. 2017; 22:594–603.
8. Waggoner JJ, Gresh L, Mohamed-Hadley A, Ballesteros G, Davila MJV, Tellez Y, Sahoo MK, Balmaseda A, Harris E, Pinsky BA. Emerg Infect Dis. 2016; 22:1295–7. [PubMed: 27184629]
9. Chen A, Wang R, Bever CRS, Xing S, Hammock BD, Pan T. Biomicrofluidics.
10. Chan K, Weaver SC, Wong PY, Lie S, Wang E, Guerbois M, Vayugundla SP, Wong S. Sci Rep. 2016; 6:38223. [PubMed: 27934884]
11. Granger D, Hilgart H, Misner L, Christensen J, Bistodeau S, Palm J, Strain AK, Konstantinovski M, Liu D, Tran A, Theel ES. J Clin Microbiol. 2017; 55:2127–2136. [PubMed: 28446573]
12. Lustig Y, Zelena H, Venturi G, Van Esbroeck M, Rothe C, Perret C, Koren R, Katz-Likvornik S, Mendelson E, Schwartz E. J Clin Microbiol. 2017; 55:1894–1901. [PubMed: 28381608]
13. Steinhagen K, Probst C, Radzimski C, Schmidt-Chanasit J, Emmerich P, van Esbroeck M, Schinkel J, Grobusch MP, Goorhuis A, Warnecke JM, Lattwein E, Komorowski L, Deerberg A, Saschenbrecker S, Stöcker W, Schlumberger W. Euro Surveill.
14. Wong SJ, Furuya A, Zou J, Xie X, Dupuis AP, Kramer LD, Shi PY. EBioMedicine. 2017; 16:136–140. [PubMed: 28094237]
15. Calvert AE, Biggerstaff BJ, Tanner NA, Lauterbach M, Lanciotti RS. PLoS One. 2017; 12:e0185340. [PubMed: 28945787]
16. Acharya D, Bastola P, Le L, Paul AM, Fernandez E, Diamond MS, Miao W, Bai F. Sci Rep. 2016; 6:32227. [PubMed: 27554037]
17. Shafiee H, Kanakasabapathy MK, Juillard F, Keser M, Sadasivam M, Yuksekkaya M, Hanhauser E, Henrich TJ, Kuritzkes DR, Kaye KM, Demirci U. Sci Rep. 2015; 5:9919. [PubMed: 26046668]
18. Saiz JC, Vázquez-Calvo Á, Blázquez AB, Merino-Ramos T, Escribano-Romero E, Martín-Acebes MA. Front Microbiol. 2016; 7:496. [PubMed: 27148186]
19. Klemm D, Heublein B, Fink HP, Bohn A. Angew Chemie Int Ed. 2005; 44:3358–3393.
20. Tobjörk D, Österbacka R. Adv Mater. 2011; 23:1935–1961. [PubMed: 21433116]
21. Sher M, Zhuang R, Demirci U, Asghar W. Expert Rev Mol Diagn. 2017; 17:351–366. [PubMed: 28103450]
22. Liana DD, Raguse B, Gooding JJ, Chow E. Sensors. 2012; 12:11505–11526. [PubMed: 23112667]
23. Yetisen AK, Akram MS, Lowe CR. Lab Chip. 2013; 13:2210. [PubMed: 23652632]

24. Lan WJ, Maxwell EJ, Parolo C, Bwambok DK, Subramaniam AB, Whitesides GM. Lab Chip. 2013; 13:4103. [PubMed: 23969547]
25. Reddy B, Salm E, Bashir R. Annu Rev Biomed Eng. 2016; 18:329–355. [PubMed: 27420573]
26. Shafiee, H., Pandya, HJ., Draz, MS., Warkiani, ME. Diagnostic devices with microfluidics. 1st. Taylor & Francis Group; 6000 Broken Sound Parkway NW, Suite 300, Boca Raton, FL 33487-2742: 2017. p. 145-161.CRC Press
27. Safavieh M, Kaul V, Khetani S, Singh A, Dhingra K, Kanakasabapathy MK, Draz MS, Memic A, Kuritzkes DR, Shafiee H. Nanoscale. 2017; 9:1852–1861. [PubMed: 27845796]
28. Shafiee H, Asghar W, Inci F, Yuksekkaya M, Jahangir M, Zhang MH, Durmus NG, Gurkan UA, Kuritzkes DR, Demirci U. Sci Rep. 2015; 5:8719. [PubMed: 25743880]
29. Faye O, Faye O, Diallo D, Diallo M, Weidmann M, Sall A. Virol J. 2013; 10:311. [PubMed: 24148652]
30. Li X, Scida K, Crooks RM. Anal Chem. 2015; 87:9009–9015. [PubMed: 26258588]
31. Sun X, Li B, Tian C, Yu F, Zhou N, Zhan Y, Chen L. Anal Chim Acta. 2018; 1007:33–39. [PubMed: 29405986]
32. Tang CK, Vaze A, Rusling JF. Anal Methods. 2014; 6:8878–8881. [PubMed: 25431626]
33. Draz MS, Shafiee H. Theranostics. 2018; 8:1985–2017. [PubMed: 29556369]
34. Draz MS, Fang BA, Zhang P, Hu Z, Gu S, Weng KC, Gray JW, Chen FF. Theranostics. 2014; 4:872–92. [PubMed: 25057313]
35. Mirabello V, Calatayud DG, Arrowsmith RL, Ge H, Pascu SI. J Mater Chem B. 2015; 3:5657–5672.
36. Draz MS, Shafiee H. Theranostics. 2018; 8:1985–2017. [PubMed: 29556369]
37. Chang TL, Tsai CY, Sun CC, Chen CC, Kuo LS, Chen PH. Biosens Bioelectron. 2007; 22:3139–3145. [PubMed: 17368015]
38. Liu X, Cheng Z, Fan H, Ai S, Han R. Electrochim Acta. 2011; 56:6266–6270.
39. Zayats, M., Willner, I., Zayats, M., Willner, I. Nanotechnology. Wiley-VCH Verlag GmbH & Co KGaA; Weinheim, Germany: 2010.
40. Rolim T, Cancino J, Zucolotto V. Biomed Microdevices. 2015; 17:3. [PubMed: 25653060]
41. Das A, Barik S, Bose A, Roy S, Biswas J, Baral R, Pal S. Immunol Lett. 2014; 162:132–139. [PubMed: 25128841]
42. Routhu NK, Byrareddy SN. J Neuroimmune Pharmacol. 2017; 12:219–232. [PubMed: 28349242]
43. Bigall NC, Härtling T, Klose M, Simon P, Eng LM, Eychmüller A. Nano Lett. 2008; 8:4588–4592. [PubMed: 19367978]

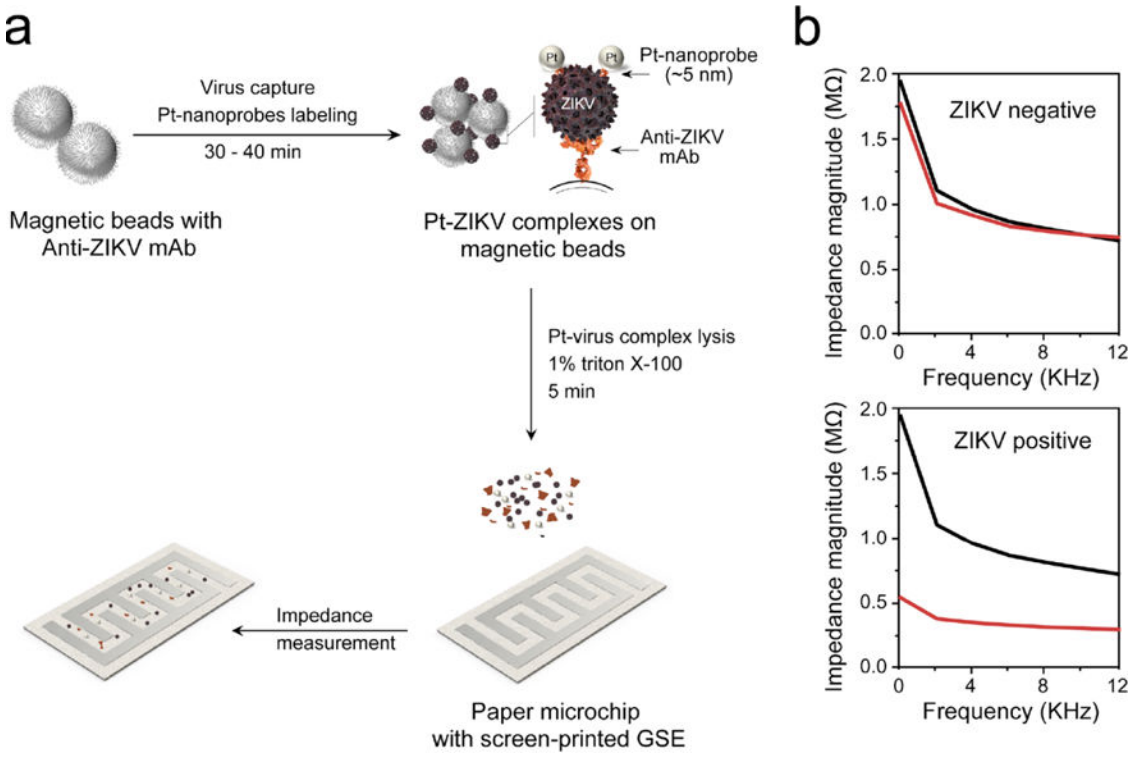

Figure 1. Schematic illustration of the developed nanoparticle-enhanced electrical sensing of Zika virus (ZIKV) on paper microchip

(a) Virus particles are captured on magnetic beads modified with ZIKV envelope monoclonal antibody (anti-ZIKV mAb) followed by labeling with specific Pt-nanoprobes (PtNP-mAb against ZIKV) forming Pt-virus complexes on the surface of magnetic beads. The Pt-virus complexes are isolated and the viral lysate/PtNPs are released using 1% Triton X-100 solution. The prepared viral lysate/PtNPs is loaded on paper microchip with screen-printed graphene-silver electrode (GSE). (b) Representative impedance magnitude measurements for ZIKV-spiked (red line) and virus-free control (black line) samples. The presence of the virus and PtNPs results in a significant change in the impedance magnitude due to the released charged viral components (*i.e.*, nucleic acid and proteins) and PtNPs.

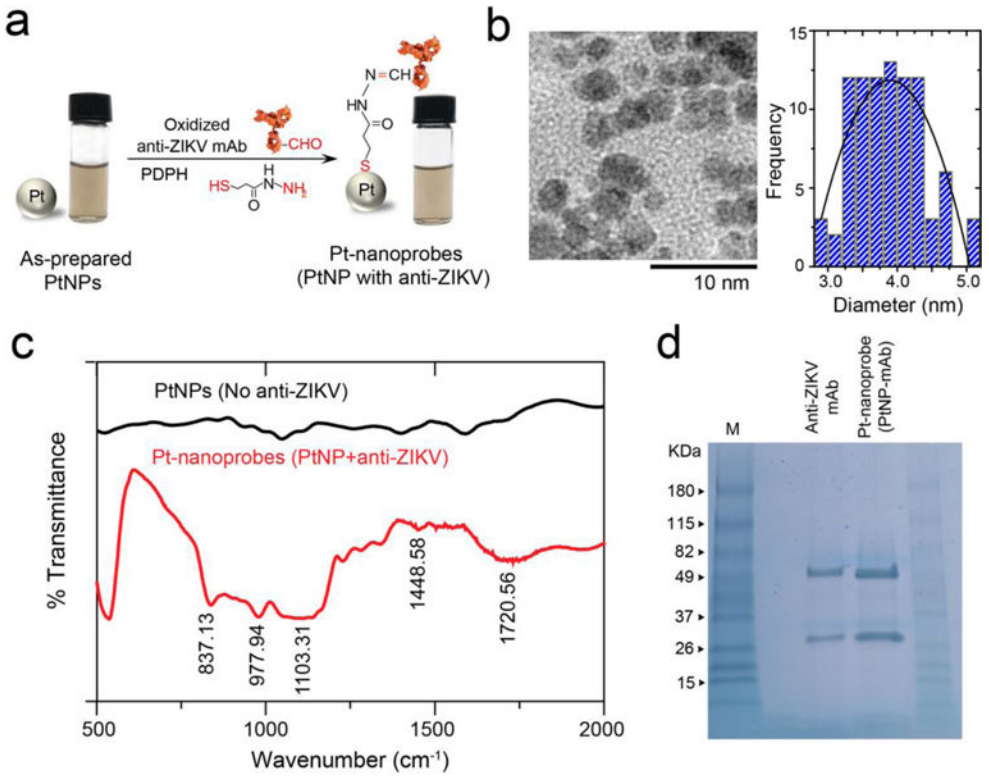

Figure 2. Pt-nanoprobe preparation and characterization

(a) Schematic illustration of the preparation reaction of Pt-nanoprobes. Oxidized anti-Zika virus monoclonal antibody (anti-ZIKV mAb) was conjugated to the surface of PtNPs using 3-(2-pyridyldithio)propionyl hydrazide (PDPH). PDPH has a thiol group that binds to PtNPs surface and a hydrazide group that binds to the free aldehyde group in the FC region of the oxidized antibody. The digital images confirm the stability of the prepared Pt-nanoprobes. (b) TEM micrograph and particle size distribution histogram of the prepared PtNPs. (c) FT-IR analysis results of PtNPs (non-modified, no antibody) and Pt-nanoprobes (PtNP-antiZIKV mAb). (d) SDS-PAGE analysis of PtNPs and Pt-nanoprobes (Pt-mAb).

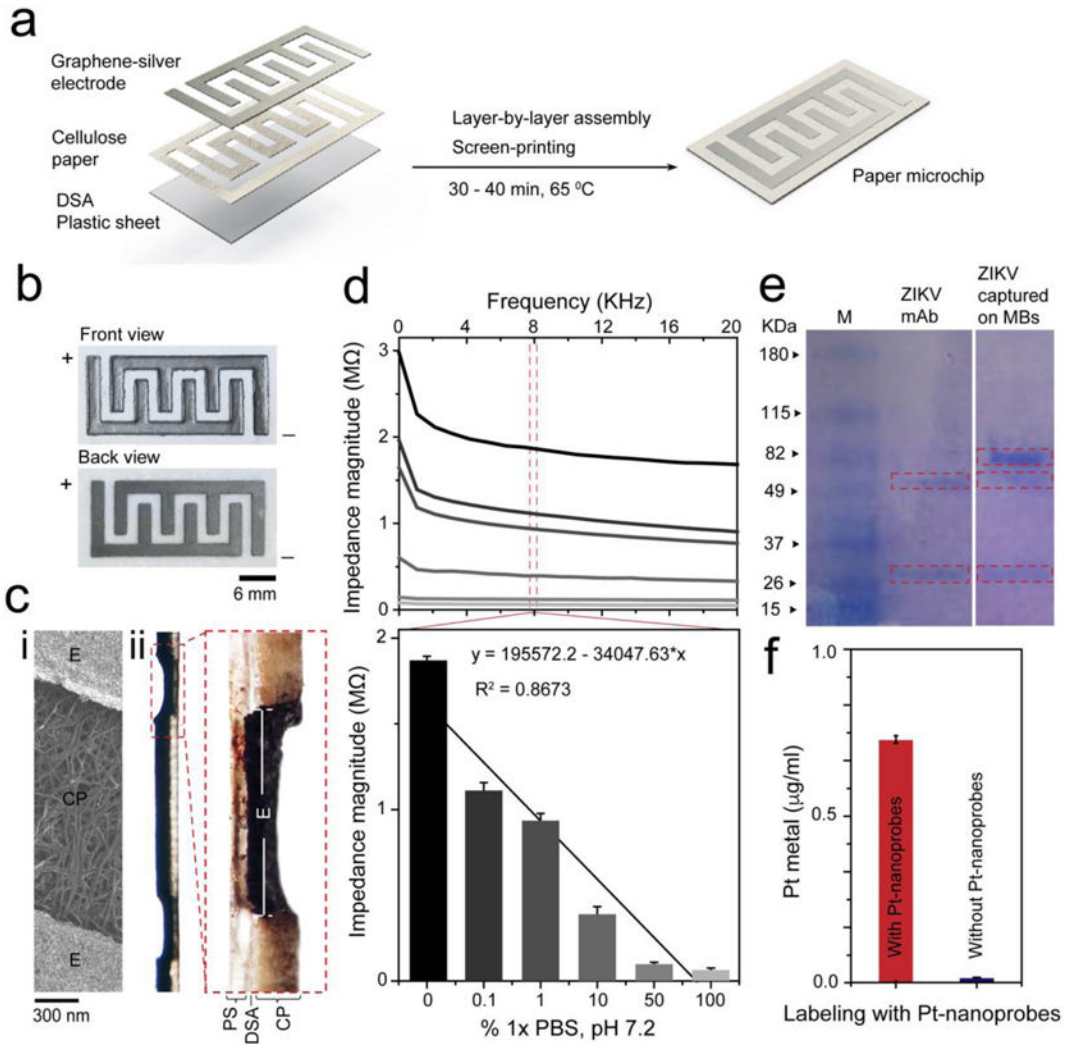

Figure 3. Paper microchip fabrication and ZIKV capture and labeling with Pt-nanoprobes

(a) Paper microchip fabrication protocol. The chip is prepared with a layer of cellulose paper (0.34 mm thickness) added to the surface of a plastic sheet by a DSA. The electrode is screen-printed on the cellulose paper using graphene-silver nanocomposite ink and then dried for 30 – 40 min at 65 0C. (b) Digital image of the prepared cellulose paper microchip. (c) SEM of the surface of the paper microchip (i) and bright-field microscopy of transverse section of the paper chip (ii). CP is cellulose paper, DSA is double-sided adhesive, E is electrode and PS is plastic sheet. (d) Average impedance magnitude spectra over a range of frequencies up to 20 KHz for different dilutions of 1× phosphate-buffer saline (PBS), pH 7.2 on the developed paper microchip. Column chart shows the correlation between the impedance magnitudes of different 1×PBS dilutions measured at 8 KHz and 1 V. (e) SDS-PAGE shows different protein bands confirming the capture of ZIKV on magnetic beads (MB). (f) Pt metal weight measured by ICP-MS confirms the labeling of ZIKV particles captured on magnetic beads using Pt-nanoprobes.

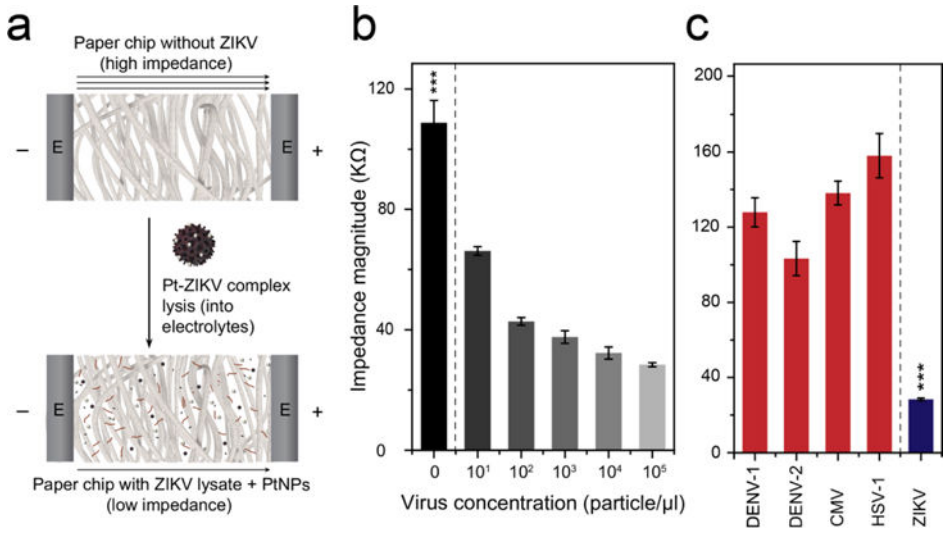

Figure 4. Performance evaluation of the developed nanoparticle-enhanced electrical sensing protocol of ZIKV on paper microchip

(a) Schematic shows the effect of the addition of viral lysate and PtNPs on the electric properties of paper microchip. (b) The detection sensitivity of ZIKV on the developed paper microchip. Different concentrations of ZIKV (101 particle/μl to 105 particle/μl) were prepared in 1× PBS and captured using magnetic beads. (c) Evaluation of the specificity of the paper chip in detecting ZIKV in the presence of non-target viruses, including dengue virus-1 and -2 (DENV-1 and -2), cytomegalovirus (CMV), and human simplex virus-1 (HSV-1). The results showed a significant decrease in the impedance magnitude of ZIKV samples compared with the tested non-target viruses. The tested virus concentration was 105 particle/μl. Error bars are standard deviations from a total of three independent measurements.

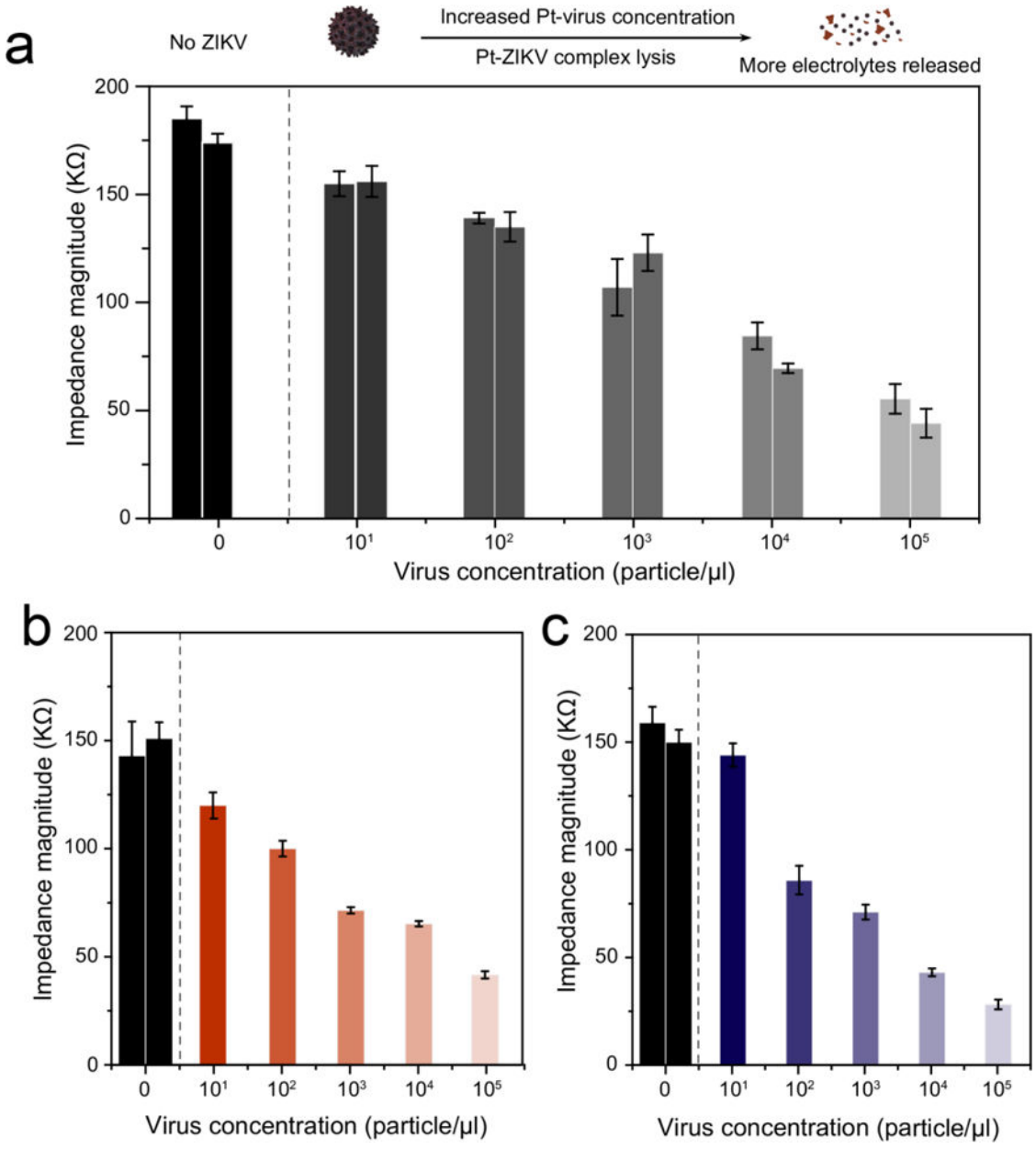

Figure 5. Detection of ZIKV in different biological fluids using the developed NP-enhanced electrical sensing on paper chip

(a) ZIKV detection in human plasma. (b) ZIKV detection in semen. (c) ZIKV detection in urine. ZIKV spiked in biological samples (101 particle/μl to 105 particle/μl) was isolated using magnetic beads and labeled with Pt-nanoprobes. The captured viruses were lysed and added to paper microchip for impedance measurement. The decrease in the impedance magnitude indicates the potential of the developed techniques for ZIKV detection in complex biological samples with a limit of detection down to 102 particle/μl. The number of the columns indicates the number of the trials performed. Error bars are standard deviations from a total of three independent measurements.